

## RESEARCH ARTICLE

# Evolutionary analysis of SARS-CoV-2 spike protein for its different clades

Matías J. Pereson<sup>1,2</sup> | Diego M. Flichman<sup>2,3</sup> | Alfredo P. Martínez<sup>4</sup> |  
Patricia Baré<sup>2,5</sup> | Gabriel H. Garcia<sup>1</sup> | Federico A. Di Lello<sup>1,2</sup> 

<sup>1</sup>Facultad de Farmacia y Bioquímica, Instituto de Investigaciones en Bacteriología y Virología Molecular (IBaViM), Universidad de Buenos Aires, Buenos Aires, Argentina

<sup>2</sup>Consejo Nacional de Investigaciones Científicas y Técnicas (CONICET), Ciudad Autónoma, de Buenos Aires, Argentina

<sup>3</sup>Instituto de Investigaciones Biomédicas en Retrovirus y Síndrome de Inmunodeficiencia Adquirida (INBIRS) – Consejo Nacional de Investigaciones Científicas y Técnicas (CONICET), Universidad de Buenos Aires, Buenos Aires, Argentina

<sup>4</sup>Virology Section, Centro de Educación Médica e Investigaciones Clínicas Norberto Quirno "CEMIC", Buenos Aires, Argentina

<sup>5</sup>Instituto de Medicina Experimental (IMEX) – Academia Nacional de Medicina, Buenos Aires, Argentina

## Correspondence

Federico A. Di Lello, Facultad de Farmacia y Bioquímica, Universidad de Buenos Aires, Junín 956, 4° piso, 1113, Ciudad de Buenos Aires, Argentina.  
Email: [fadilello@ffy.uba.ar](mailto:fadilello@ffy.uba.ar)

## Abstract

The spike protein of severe acute respiratory syndrome coronavirus 2 (SARS-CoV-2) has become the main target for antiviral and vaccine development. Despite its relevance, information is scarce about its evolutionary traces. The aim of this study was to investigate the diversification patterns of the spike for each clade of SARS-CoV-2 through different approaches. Two thousand and one hundred sequences representing the seven clades of the SARS-CoV-2 were included. Patterns of genetic diversifications and nucleotide evolutionary rate were estimated for the spike genomic region. The haplotype networks showed a star shape, where multiple haplotypes with few nucleotide differences diverge from a common ancestor. Four hundred seventy-nine different haplotypes were defined in the seven analyzed clades. The main haplotype, named Hap-1, was the most frequent for clades G (54%), GH (54%), and GR (56%) and a different haplotype (named Hap-252) was the most important for clades L (63.3%), O (39.7%), S (51.7%), and V (70%). The evolutionary rate for the spike protein was estimated as  $1.08 \times 10^{-3}$  nucleotide substitutions/site/year. Moreover, the nucleotide evolutionary rate after nine months of the pandemic was similar for each clade. In conclusion, the present evolutionary analysis is relevant as the spike protein of SARS-CoV-2 is the target for most therapeutic candidates; besides, changes in this protein could have consequences on viral transmission, response to antivirals and efficacy of vaccines. Moreover, the evolutionary characterization of clades improves knowledge of SARS-CoV-2 and deserves to be assessed in more detail as re-infection by different phylogenetic clades has been reported.

## KEYWORDS

clades, evolution, SARS-CoV-2, spike protein

## 1 | INTRODUCTION

In December 2019, the severe acute respiratory syndrome coronavirus 2 (SARS-CoV-2) emerged and shocked the entire world.<sup>1</sup> After a year of worldwide circulation, more than 98 million cases and 2 million deaths have been reported globally.<sup>2</sup> Seven genetic clades (S, L, O, V, G, GR, and GH) have been described over time that are spread throughout

different countries.<sup>3</sup> These clades represent a challenge for public health as re-infection cases with different clade strains have been reported.<sup>4–6</sup> In fact, more than 200 candidates for vaccines against SARS-CoV-2 and several antivirals are already being developed.<sup>7,8</sup> Most of the vaccines and therapeutic drugs are directed towards the spike glycoprotein (S) that is responsible for entering the host cell through recognition of the receptor ACE2 with the receptor-binding protein

(RBD).<sup>8–12</sup> Therefore, knowing the evolutionary rate of the S is relevant as changes in this protein could affect the efficacy of the vaccine and the antivirals directed to S. Even though some studies have determined the nucleotide evolutionary rate of SARS-CoV-2 using the entire genome,<sup>13,14</sup> those values are slower and do not represent the real mutation capacity of the S region alone. Only one study has reported the nucleotide evolutionary rate of the S genomic region in the first four months of the pandemic, but without differentiating the seven viral clades, which can be relevant in therapeutics and re-infections.<sup>15</sup> Thus, the aim of this study was to determine the nucleotide evolutionary rate and the haplotype network of the S region for SARS-CoV-2 in general and for each of the seven genetic clades during the first nine months of the pandemic.

## 2 | MATERIALS AND METHODS

### 2.1 | Datasets

To generate datasets representing different geographic regions and time evolution for each of the seven clades of SARS-CoV-2, from December 2019 to September 2020, the data of complete genome sequences available at GISAID (<https://www.gisaid.org/>) on September 2020 were randomly monthly collected for several geographic regions. Data inclusion criteria were: a.- complete genomes, b.- high coverage level, and c.- human host only (no other animals or environmental samples). Complete genomes were aligned using MAFFT against the Wuhan-Hu-1 reference genome (NC\_045512.2, EPI\_ISL\_402125). The resulting multiple sequence alignments were split into a data set corresponding to the S region [3822nt (21,563–25,384)] and RBD (included in S) [762nt (22,550–23,311)].

### 2.2 | Phylogenetic and genetic characterization

Patterns of genetic diversifications for both genomic regions S and RBD for each clade were analyzed using the median-joining reconstruction method with the PopART v1.7.2 software.<sup>16</sup> Haplotypes

shared among all clades were analyzed in Arlequin 3.5.2.2 software.<sup>17</sup> Polymorphism indices were calculated separately for each clade with DnaSPv. 6.12.01.<sup>18</sup>

### 2.3 | Nucleotide evolutionary rate

The estimation of the nucleotide evolutionary rate for the entire S-coding region datasets was carried out with the Beast v1.8.4 program package<sup>19</sup> at the CIPRES Science Gateway server.<sup>20</sup> The temporal calibration was established by the samples' date of sampling. The best nucleotide substitution model was selected according to the Bayesian information criterion method in IQ-TREE v1.6.12 software.<sup>21</sup> The analysis was performed under a relaxed (uncorrelated lognormal) molecular clock model recommended previously by Duchene & col.<sup>22</sup> with an exponential demographic model.<sup>23</sup> Analyses were run for  $8 \times 10^6$  generations and sampled every  $8 \times 10^5$  steps. The convergence of the “meanRate” and “allMus” parameters (effective sample size [ESS]  $\geq 200$ , burn-in 10%) was verified with Tracer v1.7.1.<sup>24</sup> The obtained substitution rate was probed against 10 independent replicates of the analysis with the time calibration information (date of sampling) randomized as described by Rieux and Khatchikian.<sup>25</sup>

## 3 | RESULTS

### 3.1 | Datasets

Three-hundred sequences were randomly selected for each clade. Two thousand and one hundred sequences were curated and selected for the analysis. Table 1 shows the SARS-CoV-2 sequences included for every month and clade.

### 3.2 | Phylogenetic and genetic characterization

The haplotype networks (Figure 1) reflect the diversity indices results as a star shape with multiple haplotypes with a few

**TABLE 1** Number of SARS-CoV-2 sequences from GISAID database on September 2020, by month and clade as per the selection criteria (temporal structure)

Clade	Dec.	Jan.	Feb.	Mar.	Apr.	May	Jun.	Jul.	Aug.	Sep.	Total
G	0	8 (2) <sup>a</sup>	20 (3)	55 (7)	52 (7)	47 (7)	39 (6)	39 (6)	20 (6)	20 (6)	300
GH	0	0	18 (3)	53 (7)	50 (7)	44 (7)	40 (7)	40 (7)	35 (6)	20 (6)	300
GR	0	0	35 (3)	45 (7)	50 (7)	40 (7)	43 (7)	35 (7)	32 (7)	20 (6)	300
L	17 (8)	43 (5)	53 (5)	65 (6)	55 (5)	49 (4)	14 (4)	4 (2)	0	0	300
O	0	35 (2)	40 (4)	55 (6)	46 (6)	42 (5)	40 (5)	24 (5)	14 (5)	4 (4)	300
S	1 (1)	50 (5)	50 (5)	70 (6)	68 (6)	31 (5)	25 (5)	4 (4)	1 (1)	0	300
V	0	4 (2)	44 (4)	101 (6)	97 (6)	33 (5)	18 (4)	2 (2)	1 (1)	0	300
<b>Total</b>	<b>18 (9)</b>	<b>140 (16)</b>	<b>260 (27)</b>	<b>444 (45)</b>	<b>418 (44)</b>	<b>286 (40)</b>	<b>219 (38)</b>	<b>148 (33)</b>	<b>103 (26)</b>	<b>64 (22)</b>	<b>2100 (300)</b>

<sup>a</sup>The number of sequences selected for the general data set (N = 300), at each moment and clade, are shown in parentheses.

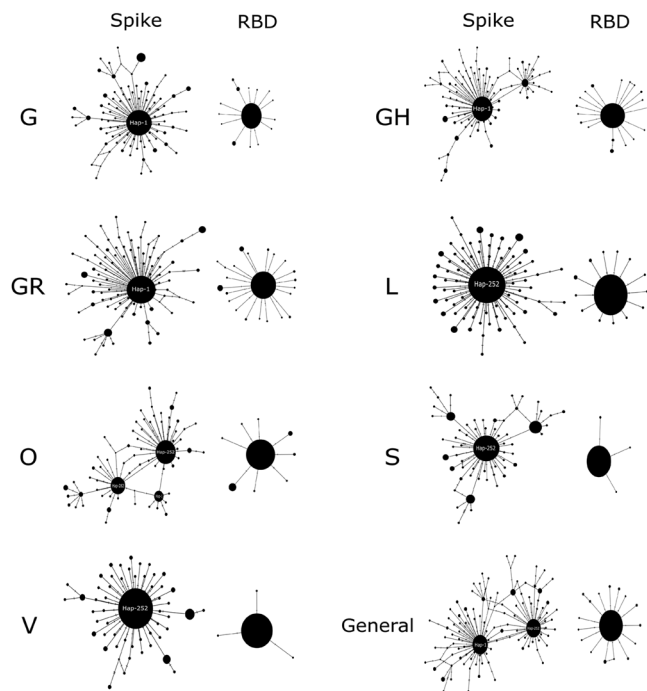


**FIGURE 1** Median-joining haplotype networks. The seven clades of severe acute respiratory syndrome coronavirus 2 (SARS-CoV-2) described to date are compared to both the entire Spike and the receptor binding protein (RBD) coding region. The diameters of the spheres are proportional to the frequency of haplotypes. The main haplogroups are indicated

nucleotide differences that diverge from a common ancestor. In all cases, the RBD diversification is lower than the spike one, being the lowest for clades S and V. For the S-coding region, 479 different haplotypes were defined in the seven analyzed clades. The number of haplotypes observed among clades ranged from 53 for the V clade to 89 for the GH and GR clades (Table 2). The major haplotype 1 (Hap-1), defined by amino acids S12, L18, R21, A222, N439, S477, T478, A522, E583, G614, Q675, E780, D936, V1068, and P1263 was the most frequent for clades G (54%), GH (54%), and GR (56%). However, other 10 haplotypes with amino acid change with respect to the Hap-1 were also observed. On the other hand, haplotype 252 (Hap-252), defined by amino acids L5, L8, H49, V367, A575, D614, A829, A846, D1084, and A1087 was the most frequent for clades L (63.3%), O (39.7%), S (51.7%), and V (70%). In addition, other 10 haplotypes showed one amino acid change with respect to Hap-252. Table 3 shows the frequency of each haplotype with amino acid changes.

The haplotype diversity was moderate to high in every clade, ranging from Hd = 0.507 to 0.793 (Table 2). In contrast, nucleotide diversity was relatively low for each clade, ranging between  $\pi = 0.0018$  for V and  $\pi = 0.0040$  for O (Table 2). Although overall diversity was similar among different clades, the haplotype and nucleotide diversities were both the lowest for V. On the other hand, haplotype and nucleotide diversity were higher for G, GH, GR, and O (Table 2). The RBD region showed indices with a similar trend but with lower values compared to the S region.

**TABLE 2** Summary of the haplotype and nucleotide diversity indices for the entire spike and the receptor binding-domain coding regions for each clade of SARS-CoV2

Clade	S	H	Hd	$\pi$
<b>SPIKE</b>				
G	100	86	0.704 ± 0.030	0.00037 ± 0.00003
GH	102	89	0.704 ± 0.030	0.00038 ± 0.00003
GR	112	89	0.683 ± 0.031	0.00038 ± 0.00003
L	87	76	0.598 ± 0.035	0.00023 ± 0.00002
O	81	68	0.793 ± 0.019	0.00040 ± 0.00002
S	72	60	0.716 ± 0.027	0.00031 ± 0.00002
V	56	53	0.507 ± 0.036	0.00018 ± 0.00002
General	134	107	0.857 ± 0.015	0.00052 ± 0.00003
<b>RBD</b>				
G	15	15	0.183 ± 0.030	0.00028 ± 0.00005
GH	17	19	0.196 ± 0.031	0.00032 ± 0.00006
GR	23	23	0.281 ± 0.034	0.00041 ± 0.00006
L	15	14	0.104 ± 0.024	0.00016 ± 0.00004
O	9	9	0.193 ± 0.030	0.00027 ± 0.00004
S	3	4	0.027 ± 0.013	0.00003 ± 0.00002
V	3	4	0.020 ± 0.011	0.00003 ± 0.00001
General	17	17	0.166 ± 0.029	0.00026 ± 0.00005

Note: S, number of variable sites; H, number of haplotypes; Hd, haplotype diversity;  $\pi$ , nucleotide diversity (per site).

### 3.3 | Nucleotide evolutionary rate

After 9 months of the pandemic, the estimated evolutionary rate for the S genomic region of SARS-CoV-2 was  $1.08 \times 10^{-3}$  nucleotide substitutions per site per year (s/s/y) (95% HPD interval  $7.94 \times 10^{-4}$  to  $1.41 \times 10^{-3}$  s/s/y). Additionally, the nucleotide evolutionary rate for the different genetic clades ranged between  $1.06 \times 10^{-3}$  and  $1.69 \times 10^{-3}$  s/s/y (Table 4). A date-randomization analysis showed no overlapping between the 95% HPD substitution-rate intervals obtained from real data and from date-randomized datasets for all clades (Figure 2).

The data set for the clade L did not reach convergence (ESS < 200). To verify the reliability of the result, 10 independent runs were performed. All of them converged in a similar posterior distribution. Likewise, for many of the random sample datasets, convergence was not achieved (ESS between 100 and 200). For those datasets that did not reach convergence, two independent runs were carried out and concatenated.<sup>26</sup>

When the evolutionary rate was analyzed according to the emergence of each clade, founding clades (L, O, S, and V) tended to present evolutionary rates slightly slower than the more recent clades (G, GH, and GR), ( $p = .157$ ).

## 4 | DISCUSSION

The evolutionary characterization of the spike genomic region of SARS-CoV-2 is crucial to estimate the course that re-infections, vaccines, and therapeutics would have in the pandemic's future. In

**TABLE 3** Frequency of haplotypes with amino acid changes in the spike for each clade of SARS-COV2

Clade/haplotype (aa change respect to Hap-1)	N (%)				Clade/haplotype (aa change respect to Hap-252)	N (%)			
	G	GH	O	GR		L	O	S	V
Hap-1 <sup>a</sup>	162 (54)	162 (54)	25 (8.3)	168 (56)	Hap-252 <sup>b</sup>	190 (63.3)	119 (39.7)	154 (51.3)	210 (70)
Hap-7 (S477N)	5 (1.7)			10 (3.4)	Hap-254 (H49Y)	3 (1)			
Hap-34 (N439K)	4 (1.3)				Hap-256 (D1084Y)	3 (1)			
Hap-67 (P1263L)	4 (1.3)				Hap-282 (NC)	6 (2)	62 (20.7)		
Hap-86 (L18F, A222V)	20 (6.8)				Hap-291 (L5F)				10 (3.3)
Hap-90 (A522S, E780C)		5 (1.7)			Hap-320 (A575S)	8 (2.6)			
Hap-91 (E780C)		6 (2)			Hap-324 (A1087S)	3 (1)			
Hap-105 (D936Y)		10 (3.4)			Hap-367 (L8V)			17 (5.7)	
Hap-137 (E583D)		3 (1)			Hap-382 (V367F)		5 (1.7)		
Hap-171 (Q675R)				3 (1)	Hap-384 (D614A)				3 (1)
Hap-187 (S12F)				3 (1)	Hap-415 (A829T)			5 (1.7)	
Hap-226 (T478I)				8 (2.6)	Hap-437 (A846S)				
Total	300 (100)	300 (100)		300 (100)	Total	300 (100)	300 (100)	300 (100)	300 (100)

Note: aa, amino acid; N, number; Hap, haplotype; NC, no amino acid changes.

<sup>a</sup>Hap-1: S12, L18, R21, A222, N439, S477, T478, A522, E583, G614, Q675, E780, D936, V1068, and P1263.

<sup>b</sup>Hap-252: L5, L8, H49, V367, A575, D614, A829, A846, D1084, and A1087.

this study, the evolutionary rate of the most important SARS-CoV-2 protein for vaccine development was estimated in general and separately for each genetic clade described in GISAID. In this context, the spike haplotype network showed a founding central paternal haplogroup from which multiple sequences with modest changes derived. Overall, the nucleotide evolutionary rate after 9 months of the pandemic was similar for each clade.

At the beginning of the pandemic, the most prevalent clades were L, O, V, and S. Later, with the appearance of the D614G mutation in the S protein, clade G emerged and remained with a high

and stable prevalence. After this initial step, the GR clade has emerged and grown until it became the most prevalent. Finally, the GH clade peaked at 30% in May 2020 and then began to decrease.<sup>3</sup> In this sense, it is important to highlight that clades with the mutation D614G in the S protein (clades G, GH, and GR) have been suggested to present a higher transmission efficiency although they would not be associated with more severe pathogenesis.<sup>27</sup>

Therefore, to describe the evolution of the S protein variants, the study of haplotypes network in all seven clades and for both regions (S and RBD alone) was performed. This analysis showed several identical sequences grouped together resulting in a star-shaped network, which is characteristic of viral outbreaks.<sup>28</sup> For the spike, this general analysis was supported by statistics that show a large number of haplotypes with a small number of nucleotide changes (low nucleotide diversity). However, for the RBD region, an increase in identical haplotypes was observed, which translates into a decrease in other parameters (H, Hd, and  $\Pi$ ). This may be due to the conserved nature of the cell receptor-binding region and is necessary for the infection of target cells. It is noteworthy that the lowest gene and nucleotide diversities observed for clade V, in both S and RBD, could be the result of fewer sequences available for this clade during the 9 months analyzed here. In this way, it can be observed that more than 90% of the V clade sequences were distributed in four months (February–May). On the other hand, the highest nucleotide diversity observed in clade O is the result of a less clearly defined pattern of mutations.<sup>29</sup>

**TABLE 4** Mean rates of the Spike-coding region (nt = 3822) for each clade of SARS-COV2

Clade	N	Model	Mean rate	HPD 95% interval
G	300	TIM2+f	$1.47 \times 10^{-3}$	$1.05 \times 10^{-3}$ – $1.95 \times 10^{-3}$
GH	300	TIM2+f+I	$1.42 \times 10^{-3}$	$9.67 \times 10^{-4}$ – $1.94 \times 10^{-3}$
GR	300	TIM2+f+I	$1.69 \times 10^{-3}$	$1.11 \times 10^{-3}$ – $2.30 \times 10^{-3}$
L	300	TIM2+f	$1.11 \times 10^{-3}$	$5.90 \times 10^{-4}$ – $1.61 \times 10^{-3}$
O	300	TIM2u+f	$1.06 \times 10^{-3}$	$7.20 \times 10^{-4}$ – $1.50 \times 10^{-3}$
S	300	TN+F	$1.33 \times 10^{-3}$	$8.41 \times 10^{-4}$ – $1.83 \times 10^{-3}$
V	300	HKY+F	$1.15 \times 10^{-3}$	$6.51 \times 10^{-4}$ – $1.64 \times 10^{-3}$
General	300	GTR+F+I	$1.08 \times 10^{-3}$	$7.94 \times 10^{-4}$ – $1.41 \times 10^{-3}$

Note: N, number of sequences.

## Spike coding region

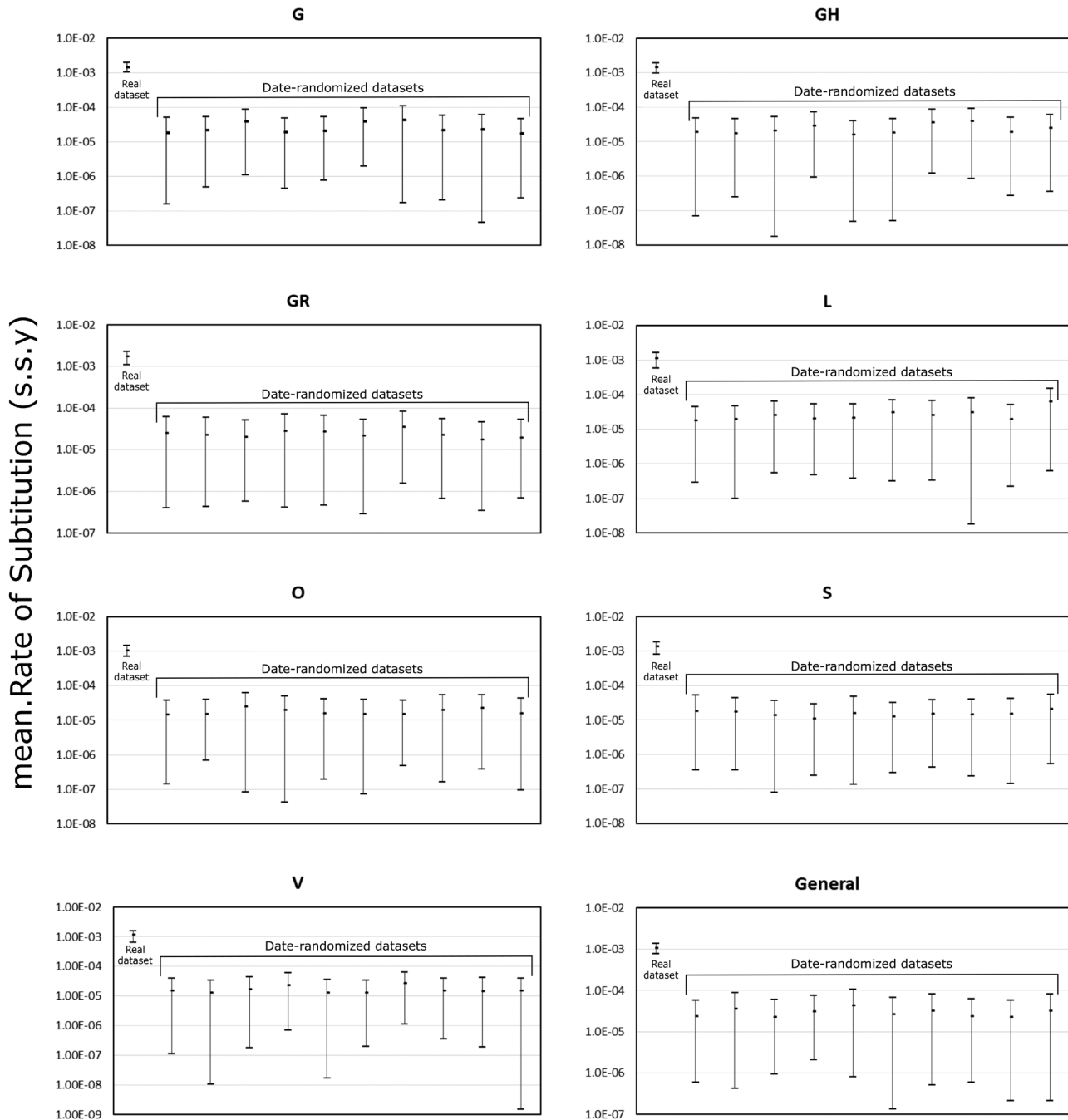


**FIGURE 2** Test of temporal structure. Comparison of the evolutionary rates estimated for the original data set versus the date-randomized ones. This analysis was performed for the Spike-coding region (3822nt) of each clade. s.s.y, substitutions/site/year

Several amino acid changes detected in the haplotypes present in our analysis are part of the RBD (V367F, S477N, N439K, T478I, and A522S). From these amino acid changes, positions 367 and 439 were associated with the binding affinity of RBD.<sup>30,31</sup> Additionally, the mutation L5F in the signal peptide was present in 3.3% of members belonging clade V.<sup>27</sup> Other changes associated to relevant functions<sup>27,30</sup> such as H49Y in clade L (associated with monomer stability), A829T in clade S (fusion peptide), D936Y in clade GH (Heptad repeat 1 [HR1] associated with monomer stability), and

P1263 in clade G (present in the cytoplasmic tail), were also detected in 1%–3.4%.

The evolutionary characterization of the wide spectrum of haplotypes contributes to determining the haplotype significance and its association with disease severity, response to antivirals, development of vaccines, and host genetic factors.

The evolutionary rate of S protein estimated for all together clades was significantly higher than that previously reported by analyzing the entire genome.<sup>14,28</sup> This is expected as the complete

genome includes several genomic regions with a high degree of conservation, while the S region is one of the most rapidly evolving in the SARS-CoV-2 genome.<sup>15</sup> Nonetheless, the spike evolution rate was quite similar to that obtained by analyzing this region during the first 4 months of the pandemic.<sup>15</sup> Although the evolutionary rate of all clades was similar, the founding clades (L, O, V, and S) showed evolutionary rates slightly lower than the most recent and currently more distributed ones (G, GH, and GR). This could be endorsed by the spread process in human populations as they are the most widely disseminated clades around the world.

This study provides substantial data on the evolutionary process of S protein in the different clades of a virus that infects a susceptible population where a massive active immunization process has not yet been carried out. However, as was aforementioned, the evolutionary rate of the S region remained stable throughout the nine considered months. In the coming months, this scenario may be modified and it would be necessary to re-evaluate the results from this study. In fact, a new clade named GV was described in the last months.<sup>32</sup> The inclusion in the study of only 2100 of the 73,393 available sequences on September 2020 is a limitation that implies a bias in the obtained results, although the sequence selection process was carefully carried out to generate a representative data set from different time courses and a wide geographic range.

## 5 | CONCLUSIONS

As the S protein of SARS-CoV-2 mediates the entry in the host cell and is the target for most therapeutic candidates, it is essential to know the manner this genomic region is evolving, given that changes in this protein could have consequences on viral transmission, response to antivirals, and efficacy of vaccines. On this basis, the results obtained in this study about the evolutionary rate of the spike protein during the first nine months of the pandemic are very significant. Furthermore, the evolutionary study of each separate clade adds to the virus knowledge and deserves to be assessed in more detail as re-infection by a different phylogenetic clade has been reported.

### ACKNOWLEDGMENTS

Matías J. Pereson, Diego M. Flichman, Patricia Baré, and Federico A. Di Lello are members of the National Research Council (CONICET). We would like to thank the researchers who generated and shared the sequencing data from GISAID (<https://www.gisaid.org/>) and Mrs Silvina Heisecke from CEMIC-CONICET for providing language assistance.

### CONFLICT OF INTERESTS

The authors declare that there are no conflict of interests.

### AUTHOR CONTRIBUTIONS

Matías J. Pereson: Data curation, acquisition of data, analysis and interpretation of data, drafting the article, final approval of the

version to be submitted. Diego M. Flichman: Data curation, Validation, drafting the article, final approval of the version to be submitted. Alfredo P. Martínez: Data curation, Validation, revising the article critically for important intellectual content, final approval of the version to be submitted. Patricia Baré: Data curation, acquisition of data, analysis and interpretation of data, revising the article critically for important intellectual content, final approval of the version to be submitted. Gabriel H. Garcia: Data curation, acquisition of data, analysis and interpretation of data, drafting the article, final approval of the version to be submitted. Federico A. Di Lello: Conception and design of the study, acquisition of data, analysis and interpretation of data, drafting the article, final approval of the version to be submitted.

### PEER REVIEW

The peer review history for this article is available at <https://publons.com/publon/10.1002/jmv.26834>

### DATA AVAILABILITY STATEMENT

Data derived from public domain resources.

### ORCID

Federico A. Di Lello  <https://orcid.org/0000-0001-9771-9705>

### REFERENCES

- Zhu N, Zhang D, Wang W, et al. A novel coronavirus from patients with pneumonia in China, 2019. *N Engl J Med*. 2020;382(8):727-733. <https://doi.org/10.1056/NEJMoa2001017>
- World Health Organization. Coronavirus disease (COVID-19) Weekly Operational Update on COVID-19. January 27, 2021. <https://www.who.int/publications/m/item/weekly-epidemiological-update-27-january-2021>. Accessed January 27, 2021.
- Alm E, Broberg EK, Connor T, et al. Geographical and temporal distribution of SARS-CoV-2 clades in the WHO European Region, January to June 2020. *Euro Surveill*. 2020;25(32):2001410. <https://doi.org/10.2807/1560-7917.ES.2020.25.32.2001410>
- Gupta V, Bhojar RC, Jain A, et al. Asymptomatic reinfection in two healthcare workers from India with genetically distinct SARS-CoV-2. *Clin Infect Dis*. 2020. <https://doi.org/10.1093/cid/ciaa1451>
- To KK, Hung IF, Ip JD, et al. COVID-19 re-infection by a phylogenetically distinct SARS-coronavirus-2 strain confirmed by whole genome sequencing. *Clin Infect Dis*. 2020:ciaa1275. <https://doi.org/10.1093/cid/ciaa1275>
- Van Elslande J, Vermeersch P, Vandervoort K, et al. Symptomatic SARS-CoV-2 reinfection by a phylogenetically distinct strain. *Clin Infect Dis*. 2020:ciaa1330. <https://doi.org/10.1093/cid/ciaa1330>
- Hu B, Guo H, Zhou P, Shi ZL. Characteristics of SARS-CoV-2 and COVID-19. *Nat Rev Microbiol*. 2020;1-14. <https://doi.org/10.1038/s41579-020-00459-7>
- World Health Organization. Draft landscape of COVID-19 candidate vaccines. November 3, 2020. <https://www.who.int/publications/m/item/draft-landscape-of-covid-19-candidate-vaccines>. Accessed November 9, 2021.
- Alexpandi R, De Mesquita JF, Pandian SK, Ravi AV. Quinolines-based SARS-CoV-2 3CLpro and RdRp inhibitors and spike-RBD-ACE2 inhibitor for drug-repurposing against COVID-19: an in silico analysis. *Front Microbiol*. 2020;11:1796. <https://doi.org/10.3389/fmicb.2020.01796>

10. Olaleye OA, Kaur M, Onyenaka C, Adebunsiyi T. Discovery of clioquinol and analogues as novel inhibitors of severe acute respiratory syndrome coronavirus 2 infection, ACE2 and ACE2–Spike protein interaction in vitro. *bioRxiv: the preprint server for biology*; 2020. 2020.08.14.250480. <https://doi.org/10.1101/2020.08.14.250480>
11. Shang J, Wan Y, Luo C, et al. Cell entry mechanisms of SARS-CoV-2. *Proc Natl Acad Sci U S A*. 2020;117(21):11727–11734. <https://doi.org/10.1073/pnas.2003138117>
12. Trezza A, Iovinelli D, Santucci A, Prischi F, Spiga O. An integrated drug repurposing strategy for the rapid identification of potential SARS-CoV-2 viral inhibitors. *Sci Rep*. 2020;10(1):13866. <https://doi.org/10.1038/s41598-020-70863-9>
13. Giovanetti M, Benvenuto D, Angeletti S, Ciccozzi M. The first two cases of 2019-nCoV in Italy: where they come from? *J Med Virol*. 2020;92(5):518–521. <https://doi.org/10.1002/jmv.25699>
14. van Dorp L, Acman M, Richard D, et al. Emergence of genomic diversity and recurrent mutations in SARS-CoV-2. *Infect Genet Evol*. 2020;83:104351. <https://doi.org/10.1016/j.meegid.2020.104351>
15. Pereson MJ, Mojsiejczuk L, Martínez AP, Flichman DM, Garcia GH, Di Lello FA. Phylogenetic analysis of SARS-CoV-2 in the first few months since its emergence. *J Med Virol*. 2020. <https://doi.org/10.1002/jmv.26545>
16. Leigh JW, Bryant D. POPART: full-feature software for haplotype network construction. *Meth Ecol Evol*. 2015;6(9):1110–1116. <https://doi.org/10.1111/2041-210X.12410>
17. Excoffier L, Lischer HE. Arlequin suite ver 3.5: a new series of programs to perform population genetics analyses under Linux and Windows. *Mol Ecol Resour*. 2010;10(3):564–567. <https://doi.org/10.1111/j.1755-0998.2010.02847.x>
18. Rozas J, Ferrer-Mata A, Sánchez-DeBarrio JC, et al. DnaSP 6: DNA sequence polymorphism analysis of large data sets. *Mol Biol Evol*. 2017;34(12):3299–3302. <https://doi.org/10.1093/molbev/msx248>
19. Suchard MA, Lemey P, Baele G, Ayres DL, Drummond AJ, Rambaut A. Bayesian phylogenetic and phylodynamic data integration using BEAST 1.10. *Virus Evol*. 2018;4(1):vey016. <https://doi.org/10.1093/ve/vey016>
20. Miller MA, Pfeiffer W, Schwartz T. *Creating the CIPRES Science Gateway for inference of large phylogenetic trees*. 2010 *Gateway Computing Environments Workshop (GCE)*. New Orleans, LA; 2010: 1–8. <https://doi.org/10.1109/GCE.2010.5676129>
21. Kalyaanamoorthy S, Minh BQ, Wong T, von Haeseler A, Jermini LS. ModelFinder: fast model selection for accurate phylogenetic estimates. *Nat Methods*. 2017;14(6):587–589. <https://doi.org/10.1038/nmeth.4285>
22. Duchene S, Featherstone L, Haritopoulou-Sinanidou M, Rambaut A, Lemey P, Baele G. Temporal signal and the phylodynamic threshold of SARS-CoV-2. *Virus Evol*. 2020;6(2):veaa061. 10.1093/ve/veaa061
23. Grassly NC, Fraser C. Mathematical models of infectious disease transmission. *Nat Rev Microbiol*. 2008;6(6):477–487. <https://doi.org/10.1038/nrmicro1845>
24. Rambaut A, Drummond AJ, Xie D, Baele G, Suchard MA. Posterior summarization in Bayesian phylogenetics using tracer 1.7. *Syst Biol*. 2018;67(5):901–904. <https://doi.org/10.1093/sysbio/syy032>
25. Rieux A, Khatchikian CE. tipdatingbeast: an r package to assist the implementation of phylogenetic tip-dating tests using beast. *Mol Ecol Resour*. 2017;17(4):608–613. <https://doi.org/10.1111/1755-0998.12603>
26. Lemey P, Salemi M, Vandamme A, eds. *The Phylogenetic Handbook: A Practical Approach to Phylogenetic Analysis and Hypothesis Testing*. 2nd ed. Cambridge: Cambridge University Press; 2009. <https://doi.org/10.1017/CBO9780511819049>
27. Korber B, Fischer WM, Gnanakaran S, et al. Tracking changes in SARS-CoV-2 spike: evidence that D614G increases infectivity of the COVID-19 virus. *Cell*. 2020;182(4):812–827. *Virus Evol*. 2020;6(2):veaa061. 10.1093/ve/veaa061 <https://doi.org/10.1016/j.cell.2020.06.043>
28. Liu Q, Zhao S, Shi CM, et al. Population genetics of SARS-CoV-2: disentangling effects of sampling bias and infection clusters. *Genomics Insights*. 2020;20:S1672–0229. <https://doi.org/10.1016/j.gpb.2020.06.001>
29. Mercatelli D, Giorgi FM. Geographic and genomic distribution of SARS-CoV-2 mutations. *Front Microbiol*. 2020;11:1800. <https://doi.org/10.3389/fmicb.2020.01800>
30. Teng S, Sobitan A, Rhoades R, Liu D, Tang Q. Systemic effects of missense mutations on SARS-CoV-2 spike glycoprotein stability and receptor-binding affinity. *Briefing Bioinform*. 2020:bbaa233. <https://doi.org/10.1093/bib/bbaa233>
31. Yi C, Sun X, Ye J, et al. Key residues of the receptor binding motif in the spike protein of SARS-CoV-2 that interact with ACE2 and neutralizing antibodies. *Cell Mol Immunol*. 2020;17(6):621–630. <https://doi.org/10.1038/s41423-020-0458-z>
32. Nextstrain: real-time tracking of pathogen evolution. [www.gisaid.org](http://www.gisaid.org). Accessed December 14, 2020.

**How to cite this article:** Pereson MJ, Flichman DM, Martínez AP, Baré P, Garcia GH, Di Lello FA. Evolutionary analysis of SARS-CoV-2 spike protein for its different clades. *J Med Virol*. 2021;93:3000–3006. <https://doi.org/10.1002/jmv.26834>